TECTONICS, VOL. 11, NO. 1, PAGES 1-11, FEBRUARY 1992

ON THE GROWTH OF NORMAL FAULTS AND THE EXISTENCE OF FLATS AND RAMPS ALONG THE EL ASNAM ACTIVE FOLD AND THRUST SYSTEM

J. P. Avouac, B. Meyer, and P. Tapponnier
Laboratoire de Tectonique, Institut de Physique du Globe de Paris, Paris

Abstract. The combination of detailed topographic leveling on the southwest segment of the El Asnam thrust fault with existing seismic and geologic data implies that the geometry of this fault involves shallow dipping flats and steep ramps. The fault appears to be growing along strike toward the southwest end, where the main shock initiated in 1980. From a depth of about 10 km, the main thrust appears to ramp to the basement-Cenozoic cover interface on a plane striking N40°E and dipping 50°-55° to the northwest. Along the southwest segment where folding has not yet developed, the thrust continues steeply through the Cenozoic cover to the near surface where it flattens, causing normal faulting. Along the central and northeast segments, which display a more evolved fold structure, the deep thrust probably flattens at a depth of 5-6 km, into a decollement along the Cenozoic-Jurassic interface before ramping to the surface. The Sara El Marouf and Kef El Mes anticlines have thus formed as fault propagation folds. Normal faults at Beni Rached probably branch with the thrust to maintain kinematic compatibility between the deep ramp and decollement. The greater separation (~7 km) between the normal faults at Beni Rached and the thrust where it crosses Oued Cheliff than along the southwest segment (~1 km) reflects the greater depth of the ramp to flat bend. We infer that the September 9, 1954, earthquake activated only the central deep segment of the main thrust together with the Beni Rached normal faults, while that of October 10, 1980, activated the whole system of flat decollements, ramp thrusts and compatibility normal faults. Further complexities of the faulting in map view are related to changes of strike of the thrust (in particular north of Oued Cheliff).

INTRODUCTION

The most active tectonic deformation in North Africa occurs in a roughly E-W trending thrust belt that has formed as a result of crustal shortening induced by the convergence between the African and European plates [e.g., McKenzie, 1972; Tapponnier, 1977]. The El Asnam fault zone belongs to that belt and has been the site of two large, recent earthquakes (September 9, 1954, Ms=6.7; October 10, 1980, Ms=7.3).

The fault plane solution of the 1954 shock [Mc Kenzie, 1972] (Figure 1) is consistent with thrust faulting, although only field evidence for normal faulting was found at the surface near Beni Rached [Rothé, 1955]. The more recent 1980 earthquake, one of the largest events recorded in northwest Africa (Ms=7.3), has been the focus of numerous seismological and geological studies. Most fault plane solutions obtained by various methods and different authors indicate thrust faulting [Ouyed et al., 1981; Cisternas et al., 1982; Deschamps et al, 1982], although Nabelek's [1985] solution also includes normal faulting.

Surface breaks show a complex pattern of thrust, bedding-parallel slip, and normal faulting, the latter having in general been interpreted as a secondary effect due to active folding [King and Vita Finzi, 1981; Yielding et al., 1981; Philip and Meghraoui, 1983] or even landsliding [Philip and Meghraoui, 1983]. Resurveying of a geodetic network and a leveling line yielded measurements of coseismic ground deformations that were generally consistent with the picture derived from the seismology and geology (i.e.; about 8 m of movement on a thrust dipping to the northwest, [Ruegg et al.,1982]). The existence of an exceptional set of reliable seismological, geodetic, and geologic data makes the El Asnam fault particularly well suited to study the geometry and mechanics of folding and thrust faulting in the upper crust.

Here, we use detailed measurements of the topography, combined with interpretations of the morphology, as well as with geological and seismological evidence to analyze the geometry and kinematics of the progressive, uneven and complex development of ramps, flats, folds, and normal faults required for geometric compatibility along the El Asnam thrust.

INCREASING COMPLEXITY OF GEOLOGICAL STRUCTURES TOWARD THE NORTHEAST, AND PROPAGATION OF THE ACTIVE FAULT AND FOLD TOWARD THE SOUTHWEST

The El Asnam thrust fault, which ruptured in 1980, is composed of three segments (Figure 1). These segments appear to be separated by seismic barriers [Yielding et al., 1981; Deschamps et al, 1982] , and probably correspond to stages of increasing shortening toward the northeast [King and Vita Finzi, 1981; King and Yielding, 1984; Meyer et al., 1990] . To the north, near Kef El Mes, one observes a well developed fold with a nearly vertical south limb (Figure 2a). In the center, the Sara El Marouf anticline is more gentle and symmetric (Figure 2b). Along the southwest segment, the fault is less marked in the morphology, and the strata do not appear to be folded: the thrust cuts a gently northwestward dipping monoclinal structure with no clear SE dips of the beds in the hanging wall (Figure

Paper number 91TC01449.
0278-7407/92/91TC-01449$10.00

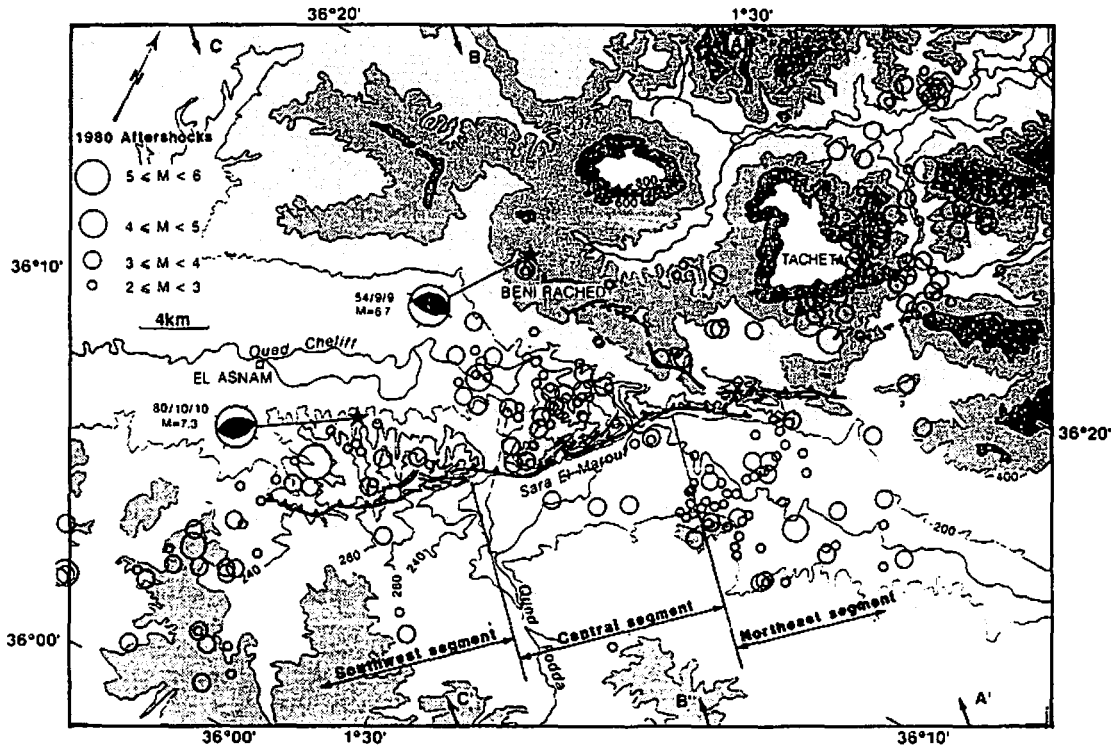

Fig. 1. Surface breaks of October 10, 1980, earthquake [after Philip and Meghraoui, 1983] reported on a topographic map. Epicentral locations and focal mechanisms of 1954 and 1980 earthquakes from McKenzie [1972] and Deschamps et al. [1982] respectively. Epicentral location of aftershocks seismicity, 5 to 37 days after the 1980 main shock, from Ouyed et al. [1981]. AA', BB', and CC' show locations of cross sections in Figures 5 and 6.

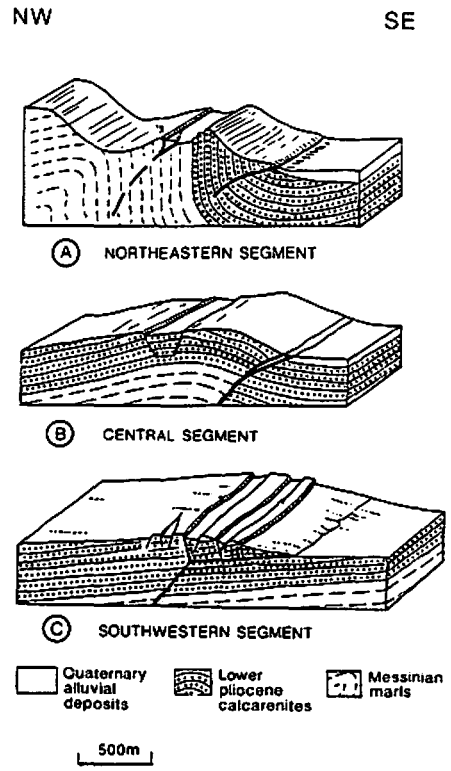

2c). Noneless the 1980 surface breaks in general closely follow the cumulative morphological expression of the fault zone (Figure 1). Hence the 1980 earthquake probably represents one of the typical increments of the deformation that has lead to the present-day topography and geological structure.

While the main thrust lies at the base of the hills it has uplifted, many surface breaks occurred on normal faults striking roughly parallel to it within these hills [Philip and Meghraoui, 1983] . Along the northern and central segments such normal faults probably result from second order extension confined to the more superficial layers. At Kef El Mes, Philip and Meghraoui [1983] present evidence that normal faulting occurs on bedding planes as a consequence

Fig. 2. Diagrammatic geological cross sections across (a) northeast, (b) central, and (c) southwestern segment of El Asnam thrust. Northeastern cross section shows a well-developed fold with steep to vertical southeast limb. Sara El Marouf anticline, in the central segment, is more gently and symmetrically folded. Finally, the thrust cuts a monoclinal structure along the southwest segment. (Figures 2a and 2b are modified from Philip and Meghraoui [1983]. Figure 2c is modified from King and Yielding [1984] and Meyer et al. [1990]

of flexural slip folding (northeast segment, Figure 2a). On top of the Sara El Marouf anticline they relate such faulting to "extrados extension" (Figure 2b). Finally, they interpret the prominent normal fault at Beni Rached to be due to large-scale landsliding (see also Ouyed et al. [1981] and Yielding et al. [1981]).

Although there is no evidence of folding along the southwest segment, normal faulting also occurs along this segment (Figure 2c). The normal faults there form a crescent-shaped zone on top of the uplifted hanging wall (Figures 1 and 3). The higher the topography, the farther that zone is from the main thrust. Conjugate "strike-slip faults" with normal components of slip connect the normal faults with the surface trace of the main thrust at an elevation of about 270 m (Figure 1) [Philip and Meghraoui, 1983]. At the junction between the southwest and central segments the fault crosses the now abandoned valley of Oued Fodda (dashed line in Figure 1), a large topographic trough with elevation under 270 m.

During field work in 1988, we made a detailed study of this area where the 1980 surface ruptures have cut and offset a small hill near the village of Zebabdja (ZH in Figure 3; also see Figure 4a). Figure 4a is a view to the east of the Zebabdja hill that was taken in January 1981. Across the field in the foreground (Figures 4a and 4d), the fault scarp, which is continuous with the well-documented thrust scarp that has offset the Algiers-Oran Railway, has a morphology compatible with high-angle reverse faulting whereas, on the side of the hill, it has a clear normal fault scarp geometry. Detailed topographic leveling (Figure 4b) supports this inference. This can be seen on the section shown in Figure 4c, where the surface trace of the fault is projected onto a vertical plane orthogonal to the fault strike. There is no interruption of the surface fault break at the transition between the normal (N) and thrust (T) faults, at an elevation of about 270 m (point P in Figures 4b and 4c). Southwestward along strike, the main thrust steps forward, to surface again along the pressure ridge zone south of Zebabdja (Figure 3). Because the lithology is principally monoclinal and gently north dipping along the southwest segment, Meyer et al. [1990] concluded that the main thrust fault abruptly splits into two faults at a stratigraphic interface, probably a marl horizon within the Pliocene calcarenite sequence (Figures 4d and 2c). The subhorizontal bedding planes guide the main thrust which flattens along them, normal faulting being required to maintain the overall compatibility of movements between hanging wall and footwall.

Extrapolating to the southwest the geometry seen at Zebabdja hill, we infer a similar geometry for most of the normal faults along the southwest segment. Where these normal faults cut across deeply entrenched valleys, they do not show any attenuation

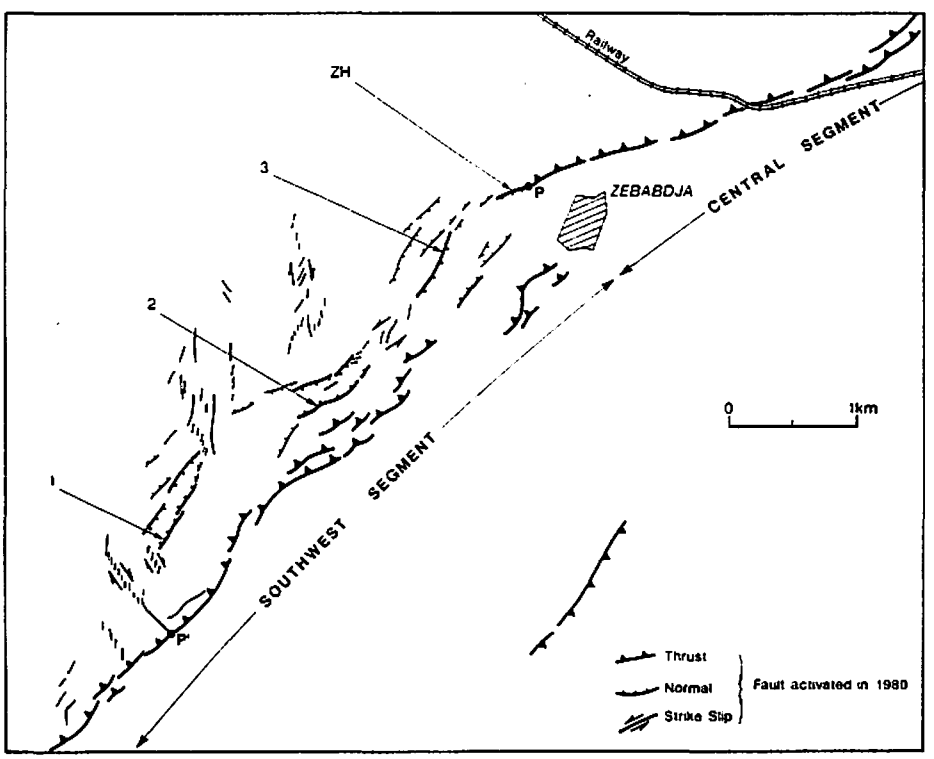

Fig. 3. Surface breaks of October 10, 1980, earthquake along the southwest segment [after Philip and Megrhaoui, 1983]. Numbers indicate sites of measurements (Figure 5 and Table 1) on normal faults [Meyer et al., 1990]. ZH is Zebabdja hill (Figure 4). Significance of points P and P' is discussed in text.

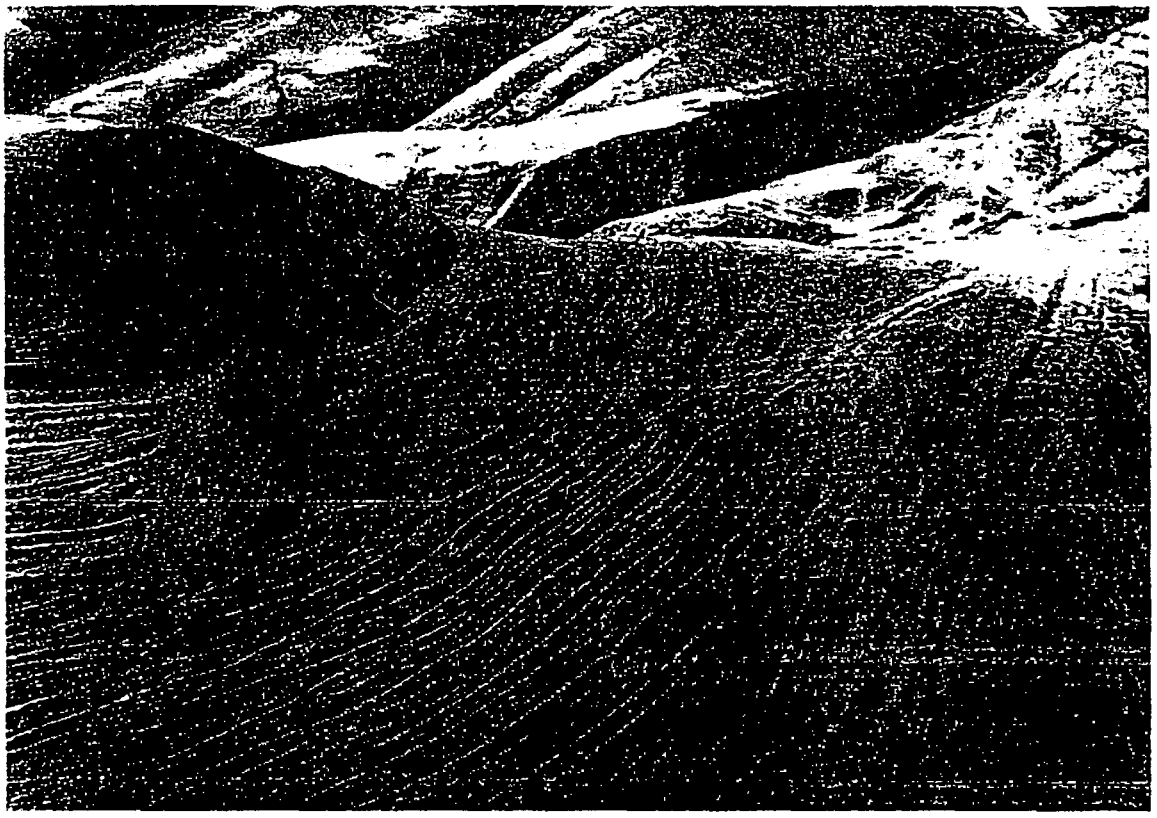

a

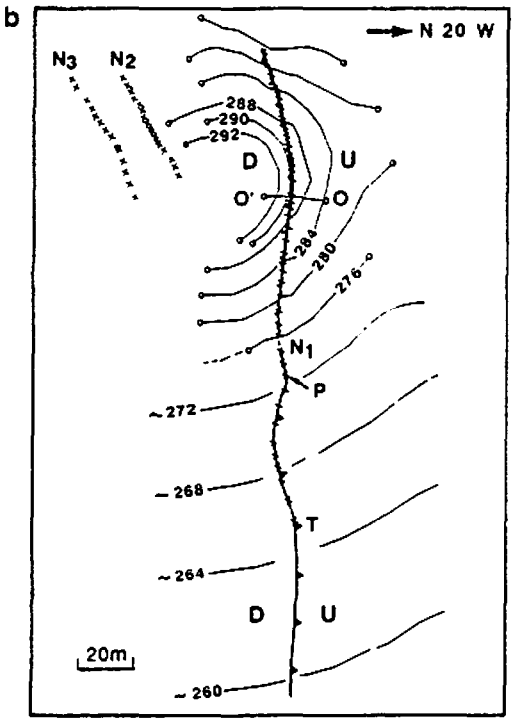

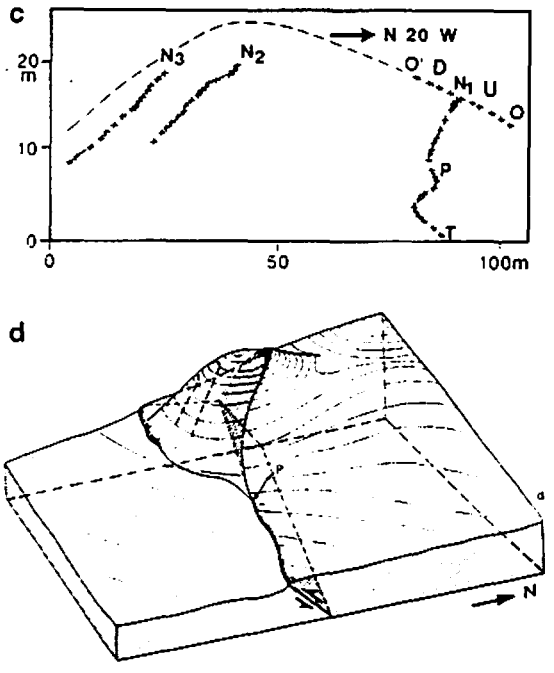

Fig. 4. At the junction between central and southwest segments, the main fault cuts and offsets a small hill near Zebabdja. (a) SW view of 1980 surface break runing across Zebabdja hill. (b) Topographic leveling around Zebabdja hill. Continuous lines are elevations contours. N and T are normal and thrust faults respectively. N1 refers to normal fault shown in Figure 4a. N2 and N3 were not activated in 1980. OO' is topographic profile orthogonal to local fault strike (N1). (c) Projection orthogonal to fault strike. No vertical exaggeration. (d) Sketch of Zebabdja hill; interpretation of fault breaks by bifurcation of main fault. P is intersection between branch line and topography (~ 270 m, see text).

with depth. Thus we suggest that these secondary faults merge with the main thrust at the place where it flattens into the bedding along a branch or bifurcation line (Figure 2c), intersecting the topography at point P and P' (Figure 3). This geometry accounts for the absence of secondary normal faults across the ancient Oued Fodda valley and at the southwest extremity of the southwest fault segment, where the topographic surface lies lower than the elevation of the branch line (Figure 1). We emphasize that such secondary faults are different from flexural slip faults, which lie parallel to the bedding, or extrados normal faults and fissures which by definition should only affect the stretched, outer strata of an anticline.

There are more normal faults at the north end of the southwest segment than farther south (Figures 1 and 3). At three sites on some of the principal faults activated uphill from that segment of the fault, we measured both the cumulative displacements recorded by offset calcarenite beds [Meghraoui, 1988] and the displacements due to the 1980 earthquake [after Meyer et al., 1990, Figures 3 and 4]. The cumulative offsets increase from 3 m to 25 m from south to north, while the 1980 offset is about the same at all three sites, between 0.8 and 1.0 m (Table 1 and Figure 5). Earthquakes comparable to that of 1980 probably rank among the largest that the El Asnam thrust fault can generate, since they rupture its entire length. The ~1 m displacement on the main southwest normal faults during the 1980 earthquake is thus probably close to the maximum possible slip during one event on these faults. None of the normal faults activated in 1980 along the southwest segment had surface scarps higher than those measured here. Hence the three normal faults on which cumulative and 1980 offsets can be compared have recorded more seismic events to the northeast than to the southwest (Table 1). Although such normal faults may be viewed as secondary, the structural sketch of Figure 2c implies that slip on them is intimately linked with slip on the main deep thrust by kinematic compatibility. Hence we infer that the entire fault system is probably older to the northeast, the cumulative offsets and morphology on the active faults resulting from more earthquakes to the north than to the south. In fact, the main thrust fault and the fold and compatibility normal faults related to it are here caught in the act of propagating southwestward. This is in keeping with the observation that the fold structure reflects more shortening progressively toward the north.

SEISMOLOGY AND GEODESY: A PATTERN SUGGESTING MULTIPLE FAULTS AND SHALLOWER, MORE DIFFUSE STRAIN TO THE NORTH

The epicentral locations determined for the main shock of the 1980 earthquake are all within 10 km of the southwest end of the fault, near the city of El Asnam, formerly known as Orleansville and now called Ech Cheliff (Figure 1) [Yielding et al., 1981; Cisternas et al., 1982]. Early studies of body waves indicated a relatively shallow hypocenter about 10 km deep [Yielding et al., 1981; Deschamps et al., 1982; Ouyed et al., 1983]. Focal mechanisms indicate (1) that the main thrust fault plane strikes between N30°E and N50°E, in rough agrement with the average N50° strike of the surface breaks, (2) that it dips between 52° and 60° towards the northwest, and (3) that the slip vector has a pitch between 83° and 90° [Ouyed et al., 1981; Yielding et al., 1981; Deschamps et al, 1982]

By modeling the first cycle of the observed P waveforms, Yielding et al. [1981] found evidence for a seismic barrier between the southwestern and central segments. They also argued that the fault plane of the southwest segment is steeper than that of the central segment. Deschamps et al. [1982] , taking into account a longer portion of the P waveform, found it necessary to include a third segment, corresponding to thrust faulting northeast of Oued Cheliff. They modeled the propagating rupture using long period body and surface waves, and they obtained a solution consisting of three breaks along the three segments in Figure 1, separated by two barriers, spanning the total length of the thrust fault (about 35 km). Studies both by Yielding et al. [1981] and Deschamps et al. [1982] showed that the rupture started at the southwest end of the fault and propagated toward the northeast. Nabelek [1985] carried out a systematic waveform inversion of P and Sh waves. He found a shallower focal depth (6 km) for the different subevents constituting the main shock and, paying particular attention to the late part of the waveforms, showed that unconstrained inversion implies normal faulting in the northeast, triggered by the incoming rupture from the southwest.

Table 1. 1980 Coseismic Offsets, Cumulative Displacements of Calcarenite Beds, and Cumulative Number of Events, Assuming Paleoseismic Displacements Comparable to That Observed in 1980

	Cumulative Normal Offset, m	1980 Normal Offset, m	Probable Number of Events
Site 1	3 ± 0.5	0.8 ± 0.1	4 ± 1
Site 2	10 ± 0.5	0.8 ± 0.1	11 ± 2
Site 3	25 ± 5	10 ± 0.1	25 ± 5

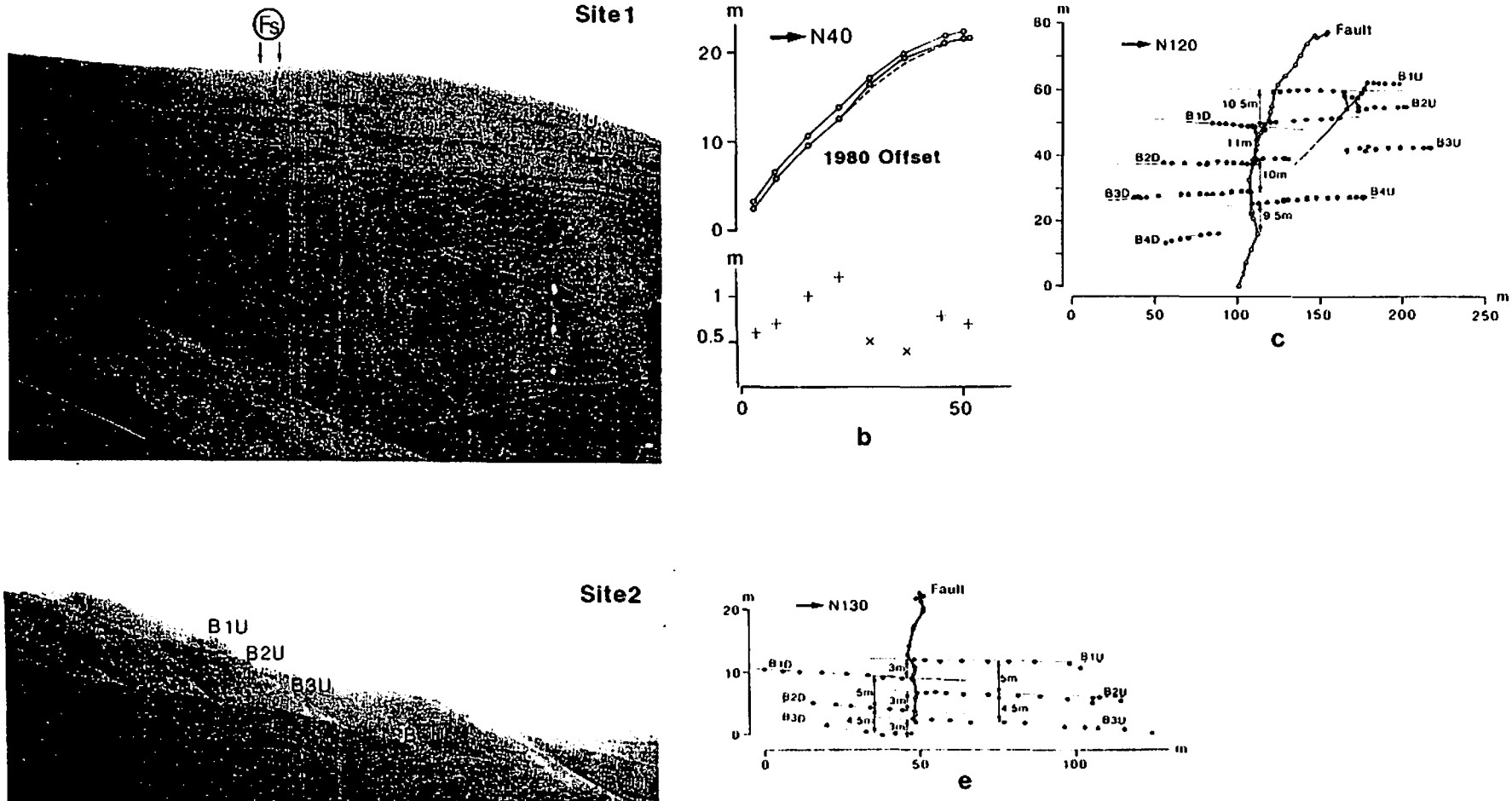

Fig. 5. (a, d, and f) NE-looking views of sites 1, 2, and 3, respectively (see Figure 3 for location). Symbols (B1, B2, etc) refer to corresponding, uplifted (U) and downthrown (D) calcarenite beds on opposite sides of the normal faults. (b) Projection along fault strike of topographic profiles running along top and bottom of 1980 fault scarp at site 1. Vertical exaggeration is 2x. Crosses represent scarp height along fault trace. (c, e, and g) Projections orthogonal to local fault strike of profiles following faults and offset calcarenite beds visible on corresponding photographs. Solid circles and open circles are for measured points along beds and faults respectively. Numbers indicate cumulative offsets (Table 1) and separation between consecutive beds on either side of faults [after Meyer et al., 1990].

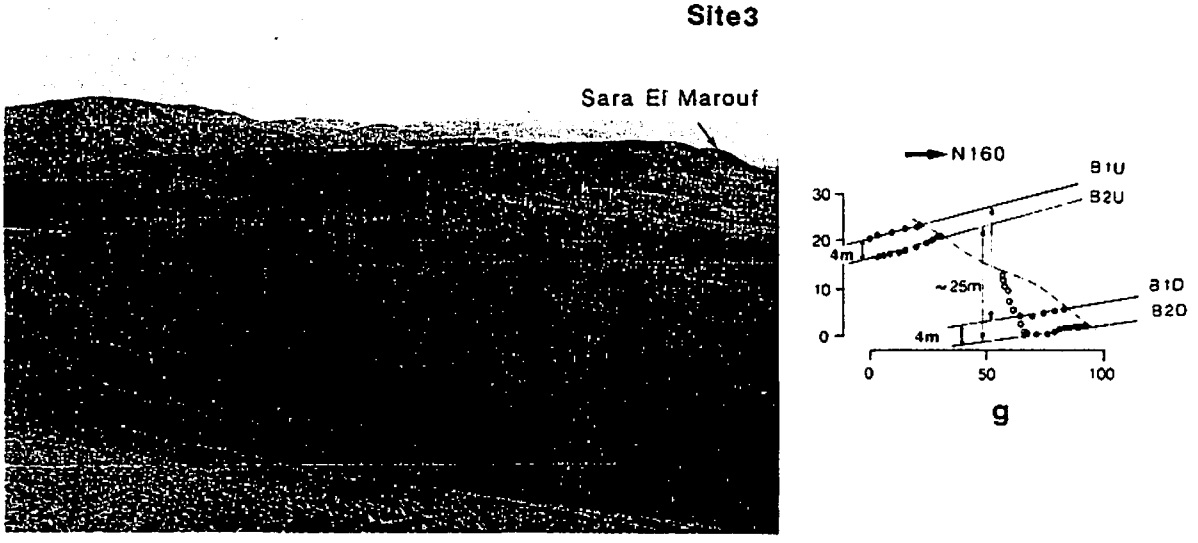

f Fig.5 (continued)

Epicentral locations of the aftershock seismicity, from 5 to 37 days after the main shock (data from Ouyed et al. [1981]), are plotted on Figure 1. Standard errors on horizontal locations are less than 2 km, and these locations do not seem to be sensitive to the velocity model [Ouyed et al., 1983]. Most aftershocks were northeast of the main shock (Figure 1) [Ouyed et al., 1983]. One outstanding feature of the data is the more diffuse and complex pattern of aftershocks in the northeast. In order to examine the vertical distribution of seismicity, hypocenters were orthogonally projected on three N130° striking cross sections spaced 15 km apart (Figure 6). Standard errors on the depth are less than 2 km [Ouyed et al., 1981] but hypocenter depths are very sensitive to the velocity model which is only weakly constrained by geological data. Consequently, mislocations of a few kilometers should be expected [Ouyed et al., 1983]. Even though the depth of the aftershocks is uncertain and must be interpreted with care, the overall pattern is insensitive to changes in the velocity model. The sections confirm the increasing complexity of the upper crustal strain release toward the northeast. On the southern cross sections (CC', Figure 6) aftershocks seem to be limited to the Mesozoic "basement" under about 6 km and may be fitted, for the most part, with a rather steeply dipping fault plane that reaches the topographic surface at the location where surface breaks were observed (solid arrow in Figure 6). Farther north, the pattern widens, a situation recalling that of the Coalinga or Kettleman Hills earthquakes [Stein and Yeats, 1989; Stein and Ekström, submitted to J. Geophys. Res.]. A peculiar cluster of events, well north of the main thrust, exists at the northern end of the aftershock zone. Cisternas et al. [1982] therefore inferred particularly complex, multiple faulting at depth there. Aftershocks on the central and northeastern sections are also shallower than on the southwestern section, most of them being scattered within the Cenozoic sedimentary cover. In fact, if one considers only the aftershocks located under about 6 km, in the Mesozoic "basement", the width of the aftershock distribution is about the same on all three sections (B. Slemmons, personal. communication, 1991). At a depth greater than about 6 km, the "basement" thrust could thus be unique and the complexity seen above 6 km probably reflects more diffuse strain associated with folding of the Tertiary sedimentary cover.

The subsurface fault geometry may also be inferred from geodesy. Geodetic networks and leveling lines were set up in the El Asnam area before the 1980 earthquake and last surveyed in 1976. In 1981, resurveying by Ruegg et al. [1982] provided measurements of horizontal and vertical deformation. The resulting strain tensor implies SE-NW shortening (about 2.5 m), uplift of the northwestern side of the fault (about 5 m) and downthrow of the edge of the underthrust block (about 1 m) [Ruegg et al.,1982, Figure 2b] . Vertical diplacements on the main thrust scarps within the network do not exceed 2.5 m [Philip and Meghraoui, 1983]. Thus the slip on the main thrust at the surface represents only a fraction of the slip at depth, which is consistent with slip being absorbed by other blind faults or by incremental folding. Ruegg et al. [1982] tested different dislocation models that could account for measured displacements, using assumptions based on seismological data. The model that fits the leveling data best involves five dislocations with different strikes (between N38°E and N67°E) and dips (between 52° and 70° to the northwest), and a slip of 8 m at depth. The southernmost segments are interpreted to dip 70° and 60° to the northwest, while northern segments are interpreted to dip 54° to the northwest. In any case, it seems that any three-dimensional model requires segmented dislocations with steeper dips in the soutwestern fault zone.

In summary, the geophysical observations are compatible with the idea that faulting started at the

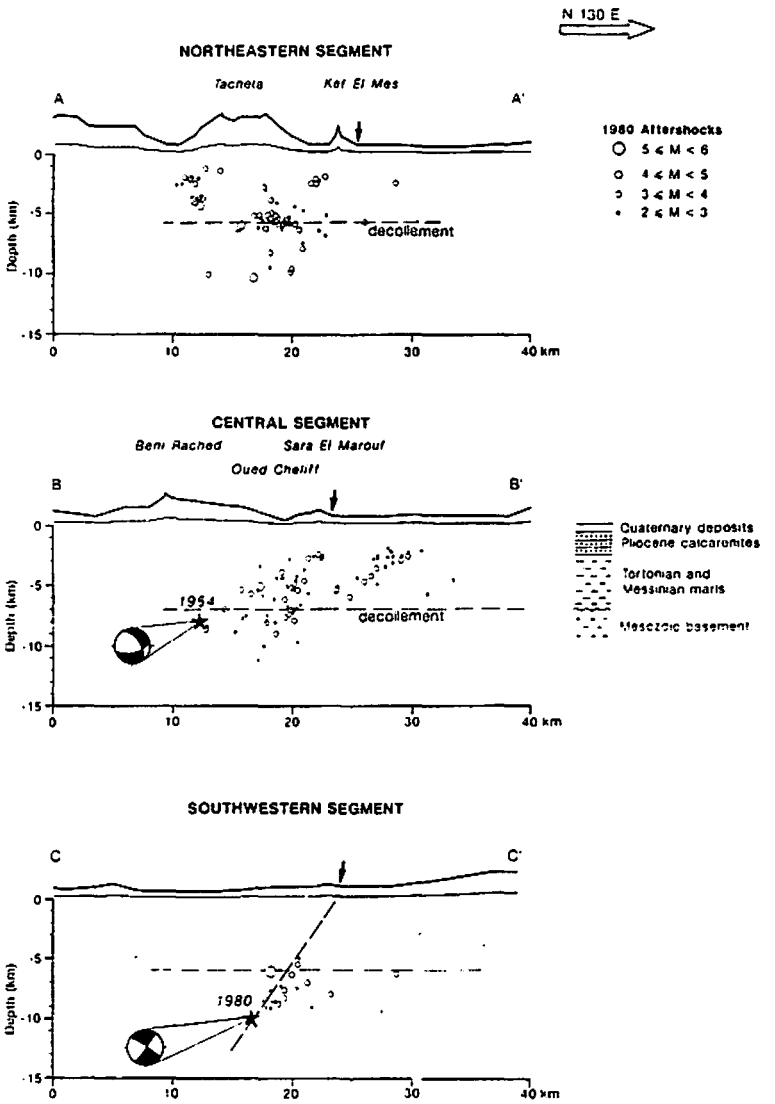

Fig. 6. Vertical projection of aftershocks on parallel cross sections AA', BB' CC' (see locations in Figure 1). Each section gathers all epicenters within 15 km wide zone centered on section. Focal mechanism and focal depth of 1980 earthquake are from Deschamps et al. [1982]. Focal mechanism of 1954 earthquake from McKenzie [1972] and focal depth from Rothé [1955]. Topograhy is shown with both no vertical exaggeration and a vertical exaggeration of 4x (above). Arrows indicate positions of thrust surface breaks. Northwest dipping dashed line on section CC' shows fault inferred from seismicity and position of surface ruptures. Dashed horizontal line roughly correponds to interface between Jurassic "basement" and Cenozoic sediments. Stratigraphic column is simplified from Meghraoui et al. [1986].

southwestern extremity of the fault zone, where we infer the tip of the laterally growing thrust fault to lie. The rupture propagated upward and northwestward, where thrusting appears to have occurred on less steeply dipping faults and where aftershocks distribution shows a more diffuse pattern of deformation at shallow depths. Only a fraction, about one third, of the slip on the thrust at depth reaches the surface along discrete scarps. The rupture process seems to be more complex where folding is more developed. According to one author [Nabelek, 1985] the last subevent in the main shock may even correspond to normal faulting along the northeast segment.

RAMP AND FLAT GEOMETRY OF THE MAIN THRUST

Although several attempts have been made to fit fault models with the geodetic or seismological data [Ouyed et al., 1981; Cisternas et al., 1982; Ruegg et al., 1982], these models involved only simple,

disconnected fault planes with different strikes and dips.

Geological and geomorphological observations suggest, however, that models involving connected flats and ramps should also be considered. There is evidence for a very shallow ramp to flat bend along the southwest segment [Meyer et al., 1990]. At a larger scale, the seismologic and geodetic evidence pertaining to the 1980 and 1954 earthquakes, the distribution of aftershocks in 1980, and the neotectonic and morphological evidence summarized here seem to be qualitatively compatible with a model involving a deeper detachement flat connecting ramps and normal faults along the central and northeast segments.

The regional stratigraphy and tectonic history makes the existence of a major detachment (or decollement) level likely. The present alluvial plains of the Cheliff valley, southeast of the fault, are remnants of an extensional Neogene basin bounded by EW normal faults that were active until middle Miocene [Meghraoui et al., 1986]. During the Miocene, the basin filled with marine sediments. Roughly N-S shortening appears to have started in the upper Pliocene, the sedimentation then becoming continental. Thus a thick layer of Mio-Pliocene sediments, with intercalated marls and sands, overlies the Mesozoic "basement" whose upper part is mostly composed of schistosed, quartzo-pelitic, Cretaceous flysch [Meghraoui et al., 1986]. According to oil exploration data, the Mio-Pliocene sediment thickness exceeds 4 km [Meghraoui et al., 1986]. The Plio-Quaternary shortening probably reactivated the Miocene normal faults as reverse faults, which may account for the steep dip of the El Asnam thrust in the "basement" [Yielding et al., 1981]. The unconformity between the Mesozoic "basement" and the Neogene cover may have localized upper crustal deformation during shortening (see stratigraphic column in Figure 6). This surface represents the most likely candidate for decoupling along a shallow dipping decollement (Figure 6).

Thus we infer that the transition in the pattern of aftershock seismicity on cross sections AA' and BB' at a deph of about 5-7 km corresponds to this "basement" cover interface. The thrust below that depth would be unique but would splay above at places within the Neogene sedimentary series, accounting for the more diffuse seismicity there (Figure 7). Along the less evolved southwest segment the main thrust probably continues steeply through the Cenozoic cover to the near surface. Along the central and northwestern segments on the other hand, the same thrust probably flattens along the Neogene-Cretaceous interface (Figures 6 and 7). The Kef El Mes and Sara El Marouf anticlines probably formed as fault propagation folds above shallower ramps climbing from this flat detachment about 5 km southeast of the "basement" thrust (Figure 7). The deep bend betwen the "basement" thrust and the decollement should have induced deformation in the overhanging block. We suspect that normal faulting at Beni Rached reflects the hanging wall compatibility strain required by such a bend (Figure 7). In fact, Beni Rached may be seen as part of a zone of topographic highs trending roughly

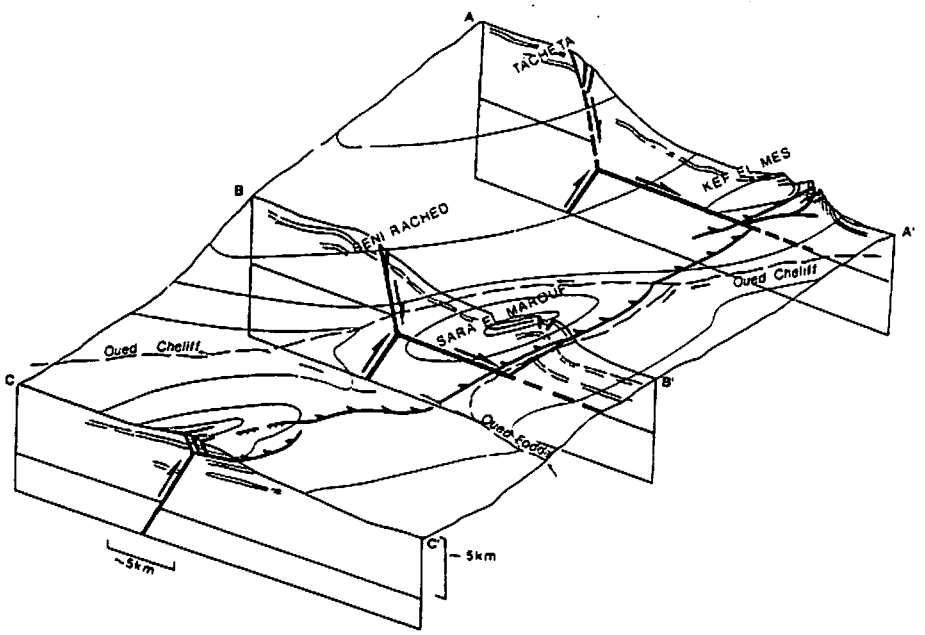

Fig. 7. Cross sections across southwestern, central, and northeastern segments of El Asnam thrust fault arranged in a three-dimensional view with schematic elevation contour lines and surface breaks. Overthrust block is shaded. The main thrust fault strikes N40°E at depth. On central and northeastern cross sections the thrust flattens at the "basement"-sediment interface. Kef El Mes and Sara El Marouf anticlines are interpreted to be fault propagation folds.

parallel to the northeast segment of the main thrust (Figure 1). This zone, which includes Djebel Tacheta, lies within the overthrust block, about 6 kilometers north of the surface thrust. It may signal uplift above a blind "basement" thrust on top of which the northern aftershock cluster occurred (Figures 1 and 6). In other words, these topographic highs could represent morphological evidence of cumulative dispacements on such a deep thrust. In 1980, normal surface breaks were actually reported along this zone [Yielding et al., 1981], but could not be accurately mapped using aerial photographs [Philip and Meghraoui, 1983], because of a dense vegetation cover. Nevertheless, the existence of such faults led Yielding et al. [1981] to propose that the 1980 earthquake activated thrust faulting under the Bled Bahari Karouch and Djebel Tacheta highs.

In summary, we infer the large scale fault geometry of the entire El Asnam thrust fault system to be similar to that seen along the southwest segment. The normal faults observed 6 km northeast of the surface trace of the thrust could merge at depth with the main thrust along a branch line at the base of the Neogene cover (Figures 6 and 7). Figure 8 shows the corresponding diagrammatic three-dimensional view. According to the hypothesis sketched in Figure 8, the large 1980 earthquake would have activated the shaded fault plane (thick line in the central segment section). The smaller 1954 earthquake would have activated only the deep, blind "basement" thrust and the normal faults at Beni Rached (dashed line in central segment section of Figure 8). Although they do not take detachement faulting into account, Cisternas et al. [1982] defend the view that normal faulting at Beni Rached in 1954 was the direct result of thrusting at depth. Their model also includes a "wedge effect" due to the change in strike of the main fault [Cisternas et al., 1982, Figure 14]. Such a wedge effect and the slight left-lateral component of movement visible along the NE striking central thrust segment and along the "en échelon" graben atop Sara El Marouf add three-dimensional complexity to the diagrams of Figures 7 and 8. But they are necessary to account for the arcuate shape of the fault pattern at Beni Rached. Changes in the fault strike at the surface are probably linked with lateral ramps, and with forward stepping of the thrust.

Overall, the geometry shown in Figures 7 and 8 results in a fault trace striking about N50°E at the surface, and a thrust striking about N40°E at depth, which fits the unconstrained fault plane solutions of Nabelek [1985]. Along the southwest segment, the thrust remains steep until the near surface. Farther north the succession of steep ramps and flats accounts for the lower average dip angle inferred from geodetical and seismological observations.

CONCLUSION

Low-angle thrust detachments are important and frequent structures in regions of crustal shortening. They are commonly seen in ancient mountains once erosion has exhumed and exposed the deep "basement" [e.g., Boyer and Elliott, 1982]. Such detachments are not well documented in zones of active thrusting however. Part of this problem arises because low-angle faults close to the earth's surface radiate seismic energy poorly. They thus contribute

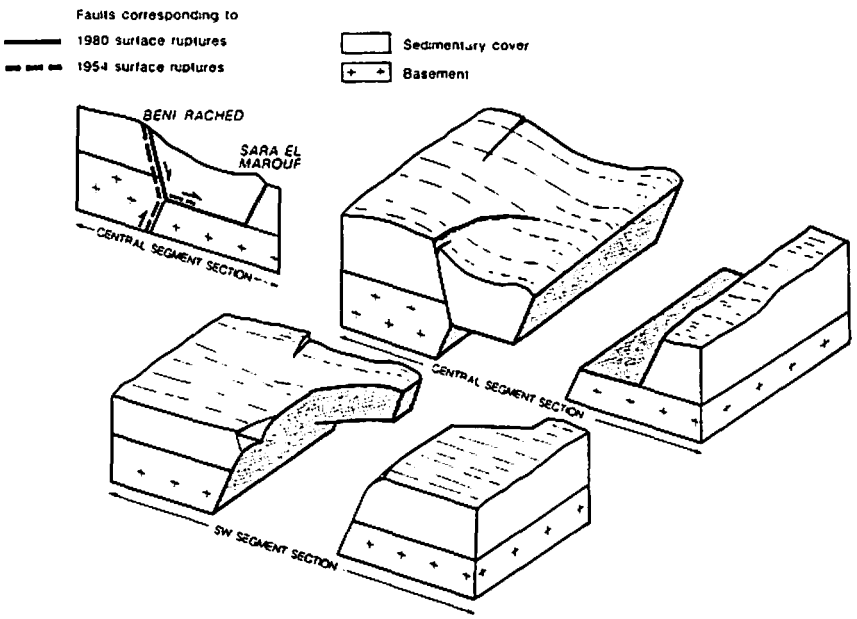

Fig. 8. Block diagram showing three-dimensional geometry of main thrust fault plane. Insert is a section of ruptured fault plane along central segment section during 1954 (dashed line) and 1980 earthquakes (bold line). See text for discussion.

only weakly to long period seismograms recorded at large distances, and thus, the proportion of the moment of an earthquake that is caused by motion on shallow low-angle planes is poorly constrained. The presence of detachments or decollements is thus difficult to establish using seismological records. Data from various origins are required to argue for the existence of such elusive subsurface structures in active fold belts.

Here, we have shown that the complexity of the surface deformations observed along the El Asnam fault zone is consistent with a complex three-dimensional geometry involving connected ramps and flats at depth. The Plio-Quaternary time sequence of faulting and folding is typified by the different stages of progressive deformation that the different thrust segments have reached. At Beni Rached, normal faults probably merge directly with the main thrust in the "basement". At Sara El Marouf and Kef El Mes, the sedimentary cover displays increasing degrees of folding. That folding probably developed as the main fault was propagating along the subhorizontal "basement"-cover interface. The Sara El Marouf and Kef El Mes folds would thus be fault propagation folds. The folded zone appears to have broadened with time in the north and center, as a result of forward propagation of the main thrust guided by stratigraphic horizons, while its southwestern tip propagated laterally.

In addition, the main thrust fault ruptured only the "basement" in 1954, merely inducing normal faulting at the surface at Beni Rached. By contrast, in 1980, the rupture propagated from the southwestern tip to activate the whole system of ramps and flats, including the normal faults already activated in 1954. The seismic cycle on the El Asnam thrust fault probably involves relatively frequent medium size earthquakes, comparable to the 1954 earthquake, and less frequent larger earthquakes such as the 1980 earthquake. Although related to deep, blind thrusting the most frequent earthquakes might induce little more than surficial normal faulting along the Beni Rached-Tacheta zone. Cumulative slip on the flat detachement ahead of this zone might be irreversibly absorbed by incremental folding or stored elastically until it is released by the large events. It would be difficult to detect without detailed studies of the morphology or without geodetic measurements. However speculative, the model of Figure 7 provides an overall framework compatible with the observed coseismic deformation (aftershock seismicity, geodesy, geometry of the surface breaks, etc.) and the finite present-day structure (topography, structural geology). Further work should aim at testing such a model with a better determination of subsurface structures from either geodesy (active fault geometry), morphology, or seismic reflection profiles.

Acknowledgments. This work was supported by the Institut National des Sciences de l'Univers (INSU) and by the Centre de Recherche d'Astronomie, d'Astrophysique et de Géophysique (CRAAG). We thank M. Meghraoui for his help in the field and D. Hatzfeld for providing the aftershocks files. We also thank B. Slemmons, who drew attention to the small width of the aftershocks zone under 6 km, one anonymous referee for constructive reviews, and Rolando Armijo for discussions. An early draft benefited from Ross Stein's comments. Special thanks are due to Guy Aveline for the illustration. This is IPGP contribution 1190.

REFERENCES

Boyer, S. E., and D. Elliott, Thrust systems, *Am. Assoc. Pet. Geol. Bull., 66*, 1196-1230, 1982.

Cisternas, A., J. Dorel, and R. Gaulon, Models of the complex source of the El Asnam earthquake, *Bull. Seismol. Soc. Am., 72*, 2245-2266, 1982.

Deschamps, A., Y. Gaudemer, and A. Cisternas, The El Asnam, Algeria, earthquake of 10 October 1980 Multiple-source mechanism determined from long- period records, *Bull. Seismol. Soc. Am., 72*, 1111-1128, 1982.

King, G. C. P., and C. Vita-Finzi, Active folding in the algerian earthquake of 10 October 1980, *Nature, 292*, 22-26, 1981.

King, G. C. P., and G. Yielding, The evolution of a thrust fault system: processes of rupture Asnam (Algeria) earthquake, *Geophys. J. R. Astron. Soc., 77*, 915-933, 1984.

McKenzie, D. P., Active tectonics of the Mediterranean region, *Geophys. J. R. Astron.Soc., 30*,109-185, 1972.

Meghraoui, M., A. Cisternas, and H. Philip, Seismotectonics of the lower Cheliff basin: Structural background of the El Asnam (Algeria) earthquake, *Tectonics, 5*, 809-836, 1986.

Meghraoui, M., Géologie des zones sismiques du Nord de l'Algérie:Thèse de Doctorat d'Etat, n°d'ordre 3945, Univ. de Paris-Sud, centre d'Orsay, Orsay, France, 1988.

Meyer, B., J. P. Avouac, P. Tapponnier, and M. Meghraoui, Mesures topographiques sur le segment SW de la zone faillée d'El Asnam et interprétation mécanique des relations entre failles inverses et normales, *Bull. Soc. Geol. Fr., 8*, 447-456, 1990.

Nabelek, J., Geometry and mechanism of faulting of the 1980 El Asnam, Algeria, earthquake from inversion of teleseismic body waves and comparison with field observations, *J. Geophys. Res., 90*, 12713-12728, 1985.

Ouyed, M., M. Meghraoui, A. Cisternas, A. Deschamps, J. Dorel, J. Frechet, R. Gaulon, D. Hatzfeld, and H. Philip, Seismotectonics of the El Asnam earthquake., *Nature, 292*, 26-31, 1981.

Ouyed, M., G. Yielding, D. Hatzfeld and G. C. P. King, An aftershock study of the El Asnam (Algeria) earthquake of 1980 October 10, *Geophys. J. R. Astron. Soc., 73*, 605-639, 1983.

Philip, H., and M. Meghraoui, Structural analysis and interpretation of the surface deformation of the El Asnam earthquake of October 10, 1980, *Tectonics, 2*, 17-49, 1983.

Rothé, J.P., Le tremblement de terre d'Orléansville et la sismicité de l'Algérie, *La Nature, 3237*, 1-9, 1955.

Ruegg J.C., M. Kasser, A. Tarantola, J.C. Lepine and B. Chouikrat, Deformations associated with the El Asnam earthquake of 10 October 1980: Geodetic determination of vertical and horizontal movements, *Bull. Seism. Soc. Am., 72*, 2227-2244, 1982.

Stein, R. S., and R. S. Yeats, Hidden earthquakes, *Sci. Am., 260 (6)*, 48-57, 1989.

Stein, R. S., and G. Eksurom, Seismicity and geometry of a 110-km-long blind thrust fault, 2, synthesis of the 1982-85 California Earthquake Sequence, submitted to J. Geophys. Res..

Tapponnier, P., Evolution tectonique du système alpin en Méditerranée: Poinçonnement et écrasement rigide plastique, *Bull. Soc. Geol. Fr., 19*, 437-460, 1977.

Yielding, G., Control of rupture by fault geometry during the 1980 El Asnam (Algeria) earthquake, *Geophys. J. R. Astron. Soc., 81*, 641-670, 1985.

Yielding, G. J. A. Jackson, G. C. P. King, H. Sinvhal, C. Vita-Finzi, and R.M. Wood, Relation between surface deformation, fault geometry, seismicity and rupture characteristics during the El Asnam (Algeria) earthquake of 10 October 1980, *Earth Planet. Sci. Lett., 56*, 287-304, 1981.

J. P. Avouac, B. Meyer, and P. Tapponnier, Laboratoire de Tectonique, Institut de Physique du Globe de Paris, 4 Place Jussieu, 75252 Paris Cedex 05, France.

(Received September 7, 1990;
revised April 23, 1991
accepted June 4, 1991)